This article has been accepted for publication in a future issue of this journal, but has not been fully edited. Content may change prior to final publication. Citation information: DOI 10.1109/JPHOT.2017.2694479, IEEE Photonics Journal

A Hollow-Core Photonic Crystal Fiber-Based SPR Sensor with Large Detection Range

Nannan Luan and Jianquan Yao

Institute of Laser and Opto-electronics, College of Precision Instrument and Opto-electronics Engineering, Key Laboratory of Opto-electronics Information Technology (Ministry of Education), Tianjin University, Tianjin 300072, China

This work was supported in part by the National Natural Science Foundation of China under Grant 61271066 and in part by the China Postdoctoral Science Foundation under Grant 2015M581296. Corresponding author: N. Luan and J. Yao (e-mail: nannanluan@gmail.com; jqyao@tju.edu.cn)

Abstract: We propose a large detection range SPR sensor based on hollow-core photonic crystal fiber in this paper. The sensor consists of an analyte channel in the core hole and a silver nanowire in the cladding holes. We investigate the resonance properties between the core modes and the surface plasmon polariton (SPP) modes excited on the nanowire surface in a large refractive index (RI) range from 1.33 to 1.5. Numerical results show that the resonance between the core mode and the higher order SPP modes can occur at particular wavelengths, thus exciting resonance peaks which shift to short wavelengths as RI increasing. By tracking most sensitive peak which is formed by the resonance combination of the *x*-polarized core mode and the second-order SPP mode, our sensor can measure large RI ranges of the analyte either higher or lower than that of the fiber material.

Index Terms: Optical fiber sensors, fiber optics.

1. Introduction

Being extremely sensitive to the refractive index (RI) of the substances on the metal surface, the surface plasmon resonance (SPR) technology has been implemented in many structures for measurement and analysis of chemical and biological analytes [1]–[4]. Among these sensing structures, the photonic crystal fibers (PCFs) based SPR sensors have shown a number of unique advantages because their various structure design [4]–[12]. In these PCF based SPR sensors [5]–[12], to realize the analyte detection, some or all of the fiber holes are coated with the metal films. The analyte can be filled into these metallized holes or their neighborhood. The surface plasmon polaritons (SPPs) can propagate at the boundary between the metal and the analyte, the incidence light can be guided in the fiber core and will be coupled with SPP modes to form the supermodes at a certain wavelength. With a strong coupling and transferring of the energy, a resonance peak is excited in the loss spectra of the transmitted light. The analyte RI change will affect the resonance condition, and thus the characteristics of the transmitted light. By following the altered characteristics of the transmitted light, the changes in the analyte RI can be detected. However, note that in these reported SPR sensors [5]–[12], the analyte is always filled into the cladding holes around the fiber core of the PCF, to keep the mechanism of total reflection, the sensor can detect only the analyte that have the RI lower than the fiber core. In the case of the silica PCF, the maximum detection value of the RI is limited to 1.42 [8]–[12]. Besides, in these designs [5]–[10], the analyte is usually filled into several adjacent holes of the PCF [5]–[10], the disturbance between these holes will introduce noises in the loss spectra of the transmitted light.

To detect and analyse high RI analytes, the SPR sensor using hollow fiber (HF) has been demonstrated both in experimental and theoretical researches [13], [14]. In these sensor designs, the liquid analyte is filled into the centre hole of the fiber to form a waveguide. When the analyte RI is higher than the material of the fiber, the incidence light can propagate in the analyte-filled waveguide to achieve the detection for high RI analyte. However, for the analyte with RI lower than the fiber material, the sensors cannot work effectively because condition of total reflection is not satisfied.

In these SPR sensors [5]–[12], the analyte directly contact with the metal. Therefore they cannot be used to detect some analytes that can generate chemical reaction with the metal. On the other hand, in practical operations, these fiber holes will be difficult to be coated with the metal films over the predefined parameters, because their sizes are very small, usually several microns. As an alternative to coating metal films, the metallic nanowire supporting the SPP modes on its surface has been demonstrated in previous works [15]–[20]. In some of the PCF-based SPR configurations [15]–[17], [19], [20], the metallic nanowire can be filled into the individual air holes to replace the metal films, and the guided light in the fiber core can couple to the SPP modes on the nanowire surface at a certain wavelength (resonance wavelength). Moreover the intensity of the coupling modes can be controlled by changing the position between the core and the nanowire [17], [20]. With a proper design, the nanowire-filled PCFs can be utilized in various applications. The metallic nanowire can be integrated into the PCF by pumping molten metal into the air holes of the fiber at high pressure, because the used metal (Au

Copyright (c) 2017 IEEE. Translations and content mining are permitted for academic research only. Personal use is also permitted, but republication/redistribution requires IEEE permission. See http://www.ieee.org/publications_standards/publications/rights/index.html for more information.

This article has been accepted for publication in a future issue of this journal, but has not been fully edited. Content may change prior to final publication. Citation information: DOI 10.1109/JPHOT.2017.2694479, IEEE Photonics Journal

or Ag) has lower melting temperature than the fiber material (silica) [15], [16], [19], [20]. In contrast to the inner coating with the thin metal films [5]–[11], which has been be fabricated by the technology of the chemical vapor deposition (CVD) [13], [21], [22], the use of nanowire provides easy operation and precise control.

In this paper, we design a PCF-based SPR sensor that has a large RI detection range. A silver nanowire is used instead of metal coating to excite the SPP modes. Different from the previous designs, a single hole in the centre hole of the PCF is filled with the analyte as the analyte channel, and its size is smaller than the cladding holes. Such design will ensure that the sensor always satisfies the condition of total reflection either at high or low analyte RI, effectively eliminates the interference by the multi-channels, and also avoids direct contact between the analyte and the silver. We investigate the coupling characteristics of the nanowire-filled FCF at different analyte RIs, and discuss the sensing performances of the sensor over a large RI detection range.

2. Structure designs and Analysis

Fig. 1 describes the schematic of the used PCF which has a hole at the core area. And the fiber core is surrounded by hexagonally arranged air holes with lattice constant Λ = 4 μm. The diameters of the center hole and the uniform cladding holes are 0.3Λ and 0.5Λ respectively. For sensor operation, a silver nanowire is filled into the air hole in the first layer as the schematic shown in Fig. 1, and an aqueous analyte is filled into the center hole. The electromagnetic mode of the proposed sensor is calculated by using the finite element method (FEM). In the numerical calculation, the RIs of the fiber material and air holes are assumed to be 1.45 (silica) and 1 respectively. The RI of the silver is given by the Drude model [23]. And the analyte RI (n_a) is changed from 1.33 to 1.5 to investigate the sensing performance.

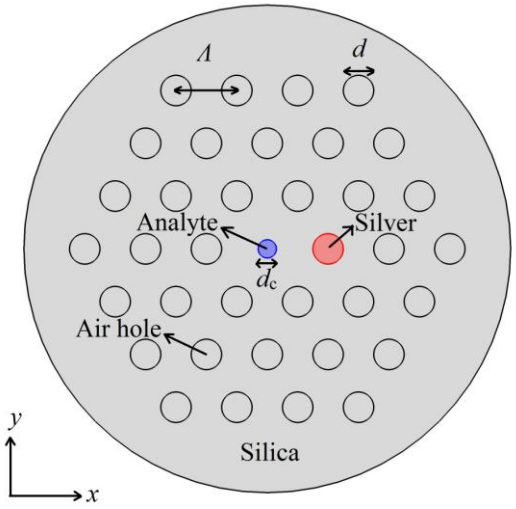

Fig. 1. Schematic of the SPR sensor based on hollow-core PCF.

According to the mode coupling theory, the core mode and the SPP mode can couple when their effective RIs (n_{eff}) are equal (phase matching) [6]–[10]. And it can be verified by an obvious peak in the core mode loss spectrum because the energy transfers to the SPP mode. To study the coupling characteristics between the core modes and SPP modes in the sensor, we plot the n_{eff} curves of the relevant modes at n_a = 1.33 in Fig. 2(a). The dashed red lines signify the SPP modes of the four mode orders excited on the silver nanowire. The solid black and dotted blue lines respectively represent the *x*-polarized (horizontally polarized) and *y*-polarized (vertically polarized) fundamental modes guided in the fiber core. The corresponding electric field (E field) distributions of these modes are illustrated in Fig. 2(b). As shown in Fig. 2(a), the fundamental and 1st order SPP modes have higher n_{eff} than the core modes, and thus cannot couple with the core modes. Whereas the higher order SPP modes (higher than 1st order) have smaller n_{eff} and can couple with the core modes when their curves intersect. Take *x*-polarized core mode for example, it can be coupled with with 2nd and 3rd SPP modes at the intersections (phase matching points) A and B, respectively. This phenomenon can be also recognized from the insets A and B in Fig. 2(b) that the core modes interact with the corresponding SPP modes, thus forming the supermodes. As the energy from the core modes coupling to the relevant SPP modes, high losses in the spectra of the core modes will be appeared at the corresponding phase matching points, shown in Fig. 3.

1943-0655 (c) 2016 IEEE. Translations and content mining are permitted for academic research only. Personal use is also permitted, but republication/redistribution requires IEEE permission. See http://www.ieee.org/publications_standards/publications/rights/index.html for more information.

This article has been accepted for publication in a future issue of this journal, but has not been fully edited. Content may change prior to final publication. Citation information: DOI 10.1109/JPHOT.2017.2694479, IEEE Photonics Journal

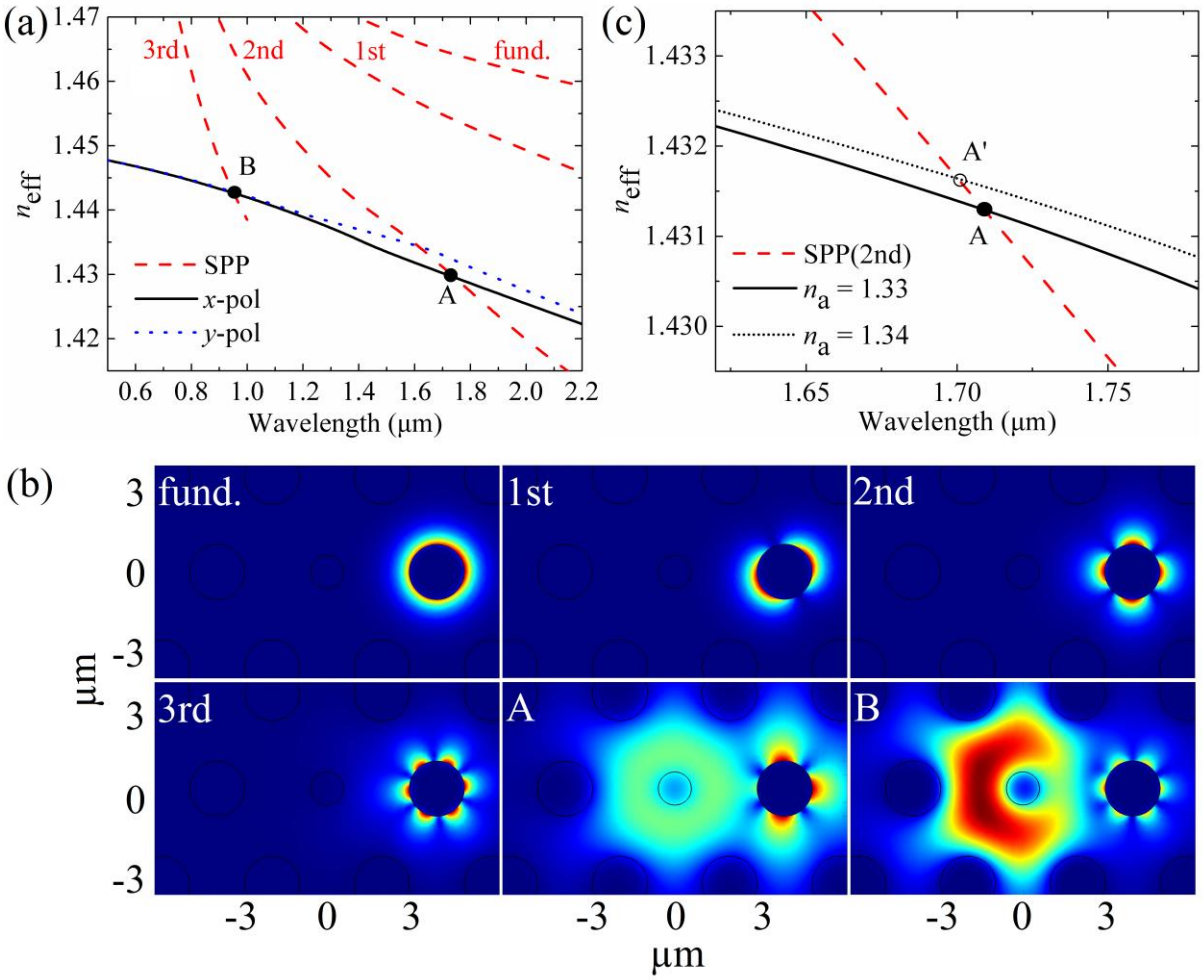

Fig. 2. (a) Effective RI (n_{eff}) curves of the core modes and the SPP modes at n_a = 1.33. (b) Electric field distributions of the *x*-polarized fundamental, 1st order, 2nd order, 3rd order SPP modes, and *x*-polarized core modes at phase matching points A and B. (c) The n_{eff} curves of the *x*-polarized core modes and the 2nd order SPP modes at n_a = 1.33 and 1.34.

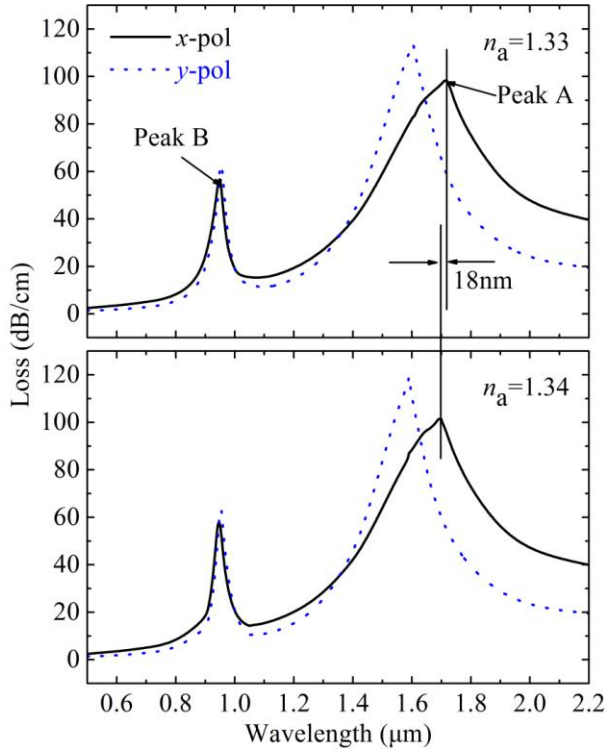

Fig. 3. Loss spectra of the two polarized core modes of the sensor at n_a = 1.33 and 1.34.

1943-0655 (c) 2016 IEEE. Translations and content mining are permitted for academic research only. Personal use is also permitted, but republication/redistribution requires IEEE permission. See http://www.ieee.org/publications_standards/publications/rights/index.html for more information.

This article has been accepted for publication in a future issue of this journal, but has not been fully edited. Content may change prior to final publication. Citation information: DOI 10.1109/JPHOT.2017.2694479, IEEE Photonics Journal

3. Results and Discussion

The n_a variation will change the n_{eff} of the relevant modes, and thus their phase matching points (resonance peaks). Consequently, by tracking shifts of the resonance peaks, the n_a changes can be measured. Fig. 3 shows the loss spectra of the core modes when the n_a is slightly varied from 1.33 to 1.34. The losses of the core modes are proportional to the imaginary part of the n_{eff} and can be estimated by [11], [12]

$$\alpha_{loss} = 10 \lg e \cdot 2k_0 \, \mathrm{Im}[n_{eff}] = 8.686 \cdot k_0 \, \mathrm{Im}[n_{eff}] \qquad (1)$$

here $k_0 = 2\pi/\lambda$ is the wavenumber with λ being the free-space wavelength. As shown in Fig. 3, the second *x*-polarized peak (Peak A) formed by the *x*-polarized core mode and the 2nd SPP mode is more sensitive to the n_a changes, because the core mode with the E field predominantly orthogonal to the silver surface can couple to surface plasmons more readily [24], [25]. The peak A shifts 18 nm ($\Delta\lambda_{peak}$) for the n_a changing from 1.33 to 1.34 (Δn_a). And the corresponding sensitivity in terms of the refractive index unit (RIU) is 1800 nm/RIU, which is normally defined as [7], [9]

$$S(\mathrm{nm/RIU}) = \Delta\lambda_{peak} / \Delta n_a \qquad (2)$$

The sensitivity obtained here is comparable to that of the previous PCF SPR sensors at the same n_a [5], [9]. Note that the resonance peak in this sensor moves toward shorter wavelengths as n_a increasing. This behavior is contrary to that in previous sensor designs which the peaks move to longer wavelengths [5]–[12]. The difference of the peak behavior is caused by the analyte filling positions. In this sensor, the analyte is filled into the hole at the fiber core. The n_a increasing will increase directly the n_{eff} curve of the core mode, as shown in Fig 2(c), and making the intersection (phase matching point) shifts from A to A'. On the contrary, in the previous SPR sensors [5]–[12], the analyte is filled into the holes at the fiber cladding. And the n_a increasing could increase the n_{eff} curve of the SPP mode, and resulting in the phase matching point moving to longer wavelengths. The abnormal behavior of resonance peak in here is also consistent to that in the other sensors with the same filling position [13], [14].

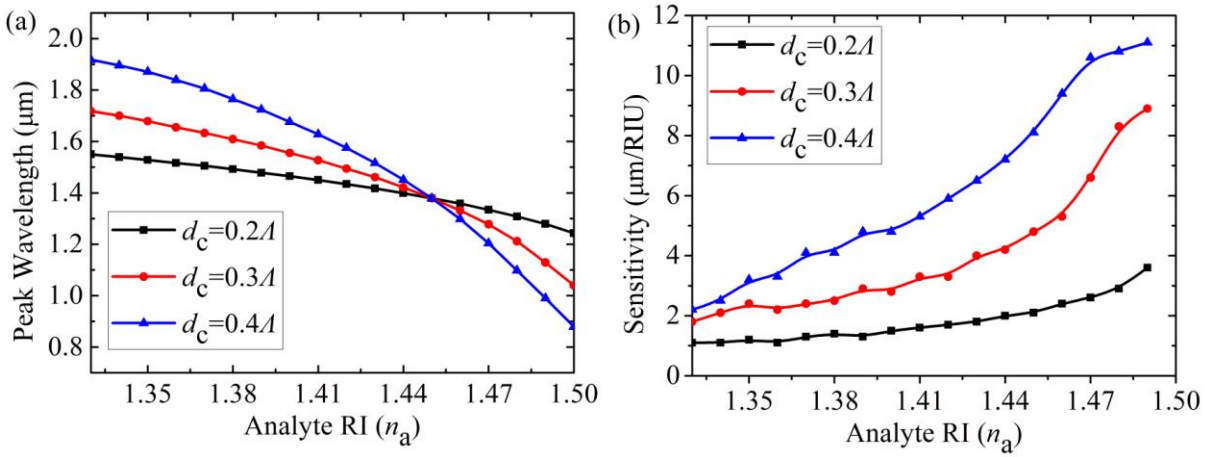

Fig. 4. The peak wavelengths (a) and the sensitivities (b) of the second *x*-polarized peak at different n_a when the fiber central hole (analyte channel) diameter (d_c) are 0.2Λ, 0.3Λ, 0.4Λ.

The diameter of the hole at the fiber core (analyte channel) is smaller than that of the cladding holes, which make the fiber core has a higher average RI than the cladding in a large n_a range, and thus satisfying the condition of total reflection. To demonstrate potential of the proposed sensor for a large n_a range sensing, we focus on the second *x*-polarized peak (Peak A) as an example and calculate its loss spectra at different n_a to find the corresponding resonance wavelengths. The results are presented in Fig. 4(a). By following the Peak A, we present the corresponding sensitivities in terms of refractive index units (RIU) in Fig. 4(b). The resonance peak of this sensor has a larger shift at high n_a, and thus a higher sensitivity. This performance is consistent with other low RI SPR sensors [8]–[12], but caused by different mechanism. To clearly explain the sensing mechanism, we illustrate the E field distributions of the *x*-polarized core modes at the non-resonance wavelength 0.6 μm for the case when the n_a is 1.4, 1.45, and 1.5 in Fig. 5(a)–(c). At the n_a lower than the fiber material RI, as shown in Fig. 5(a), the core mode is confined mainly in the core region around the analyte channel (center hole). As n_a increasing, the confinement of the core mode becomes weaker, and more evanescent wave will penetrate into the analyte channel, thus increasing the sensitivity. In this case, the higher sensitivity is caused by the extension of evanescent wave, which is also the same as in previous SPR sensors with analyte filling into the cladding holes [8]–[12]. However, when the n_a is higher than the fiber RI, the core mode is located mostly at the analyte channel in the core region as shown in Fig. 5(c). The increasing n_a will restrict more energy of the core mode at the analyte channel area, and resulting in a higher sensitivity. In this situation, the sensitivity is affected by the restricted degree of the core mode. In the process of the n_a increasing, the energy of the core mode is always confined in the core area, and gradually concentrate in the analyte channel as the E field distributions shown in Fig. 5(a)–(c). Additionally, when the n_a is high enough, the core mode is mostly confined at the analyte channel. And this will actually increase the distance between the core mode and the SPP mode and reduce the coupling strength between them, which can be seen from E field distributions of the core resonance modes at Peak A in Fig. 5(d)–(f).

1943-0655 (c) 2016 IEEE. Translations and content mining are permitted for academic research only. Personal use is also permitted, but republication/redistribution requires IEEE permission. See http://www.ieee.org/publications_standards/publications/rights/index.html for more information.

This article has been accepted for publication in a future issue of this journal, but has not been fully edited. Content may change prior to final publication. Citation information: DOI 10.1109/JPHOT.2017.2694479, IEEE Photonics Journal

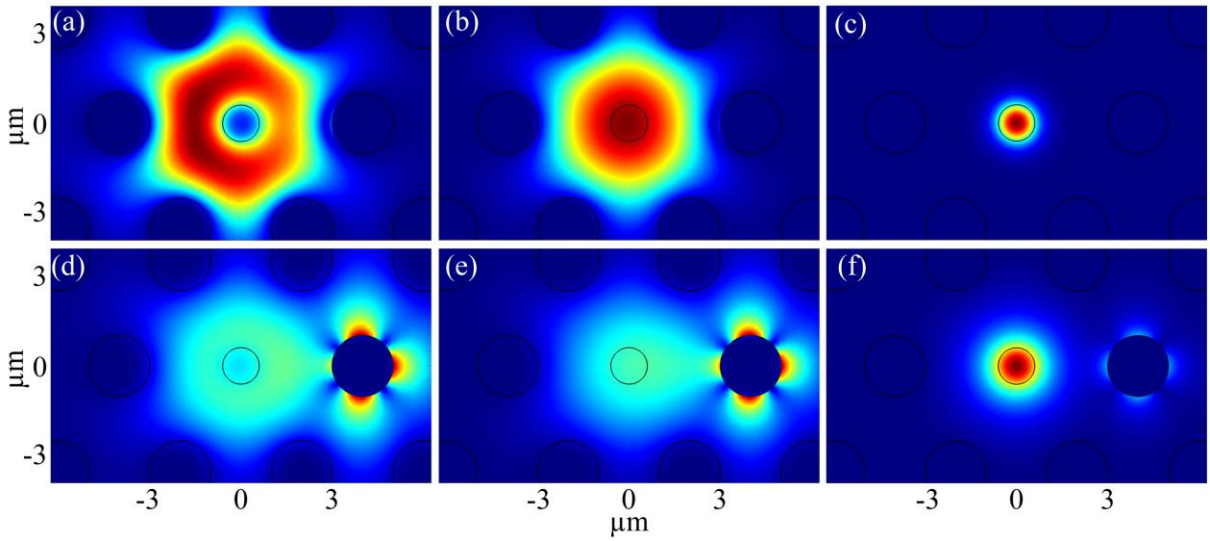

Fig. 5. Electric field distributions of the *x*-polarized core modes when (a) n_a = 1.4, λ = 0.6 μm; (b) n_a = 1.45, λ = 0.6 μm; (c) n_a = 1.5, λ = 0.6 μm; (d) n_a = 1.4, λ = 1.555 μm; (e) n_a = 1.45, λ = 1.379 μm; (f) n_a = 1.5, λ = 1.04 μm.

In Figs. 4(a) and 4(b), we also present the resonance wavelengths and the sensitivities of the Peak A at different n_a when the diameters of the analyte channel (d_c) are 0.2Λ and 0.4Λ, respectively. In Fig. 4(a), we can observe that the resonance wavelength is longer for the larger d_c at low n_a, and as n_a increasing, the resonance wavelength becomes smaller. This phenomenon can be explained by the fact that the larger size of the analyte channel (d_c) increases the proportion of the analyte in core area and promotes the capacity of changing core mode n_{eff}. At low n_a, the larger d_c can effectively reduce the n_{eff} of the core mode, and leading to its curve intersected with the SPP mode at longer wavelengths. At high n_a, the larger d_c can more rise the n_{eff} of the core mode, and resulting in the curves crossed at shorter wavelengths. When the n_a is 1.45, the analyte is index matched with the fiber material. The sensor becomes immaterial what d_c is considered. Hence its resonance wavelength is not changed even if the d_c is changed, as shown in Fig. 4(a). Because the larger d_c can change the n_{eff} of the core mode more effectively, the sensor with larger d_c can provide higher sensitivity as shown in Fig. 4(b). Concerning the practical operations, larger analyte channel (d_c) will also facilitate the analyte filling process.

4. Conclusion

In this paper, we design a large RI detection range SPR sensor based on hollow-core PCF filled with a silver nanowire. The single hole in the fiber core as the analyte channel can make the sensor has a large detection range and also eliminates the interference between neighboring analyte channels. The silver nanowire filling into the cladding hole can support SPP modes around its surface and also avoids metal coating. Simulation results demonstrate that the proposed sensor can work effectively in RI range from 1.33 to 1.5 and shows higher sensitivity at large size of the analyte channel (d_c). Moreover, to ensure the sensor can work at any value of analyte RI, the d_c should be smaller than the cladding holes. And this should be concerned when fabricating or choosing the PCF. The design presented here avoids direct contact between the analyte material and the silver. And it is expected to be recoverable after each operation.

References

[1] J. Homola, S. S. Yee, and G. Gauglitz, “Surface plasmon resonance sensors: Review,” *Sens. Actuators B, Chem.*, vol. 54, no. 1, pp. 3–15, Jan. 1999.
[2] J. Homola, “Surface plasmon resonance sensors for detection of chemical and biological species,” *Chem. Rev.*, vol. 108, no. 2, pp. 462–493, 2008.
[3] M. Couture, S. S. Zhao, and J. F. Masson, “Modern surface plasmon resonance for bioanalytics and biophysics,” *Phys. Chem. Chem. Phys.*, vol. 15, no. 27, pp. 11190–11216, Jun. 2013.
[4] Y. Zhao, Z, Deng, and J. Li, “Photonic crystal fiber based surface plasmon resonance chemical sensors,” *Sensor. Actuators B, Chem.*, vol. 202, pp. 557–567, Oct. 2014.
[5] M. Hautakorpi, M. Mattinen, and H. Ludvigsen, “Surface-plasmon-resonance sensor based on three-hole microstructured optical fiber,” *Opt. Express*, vol. 16, no. 12, pp. 8427–8432, Jun. 2008.
[6] A. Hassani and M. Skorobogatiy, “Design criteria for microstructured-optical-fiber-based surface-plasmon-resonance sensors,” *J. Opt. Soc. Amer. B*, vol. 24, no. 6, pp. 1423–1429, Jun. 2007.
[7] B. Gauvreau, A. Hassani, M. F. Fehri, A. Kabashin, and M. Skorobogatiy, “ Photonic bandgap fiber-based surface plasmon resonance sensors,” *Opt. Express*, vol. 15, no. 18, pp. 11413–11426, Sep. 2007.
[8] X. Yu, Y. Zhang, S. Pan, P. Shum, M. Yan, Y. Leviatan, and C. Li, “A selectively coated photonic crystal fiber based surface plasmon resonance sensor,” *J. Opt.*, vol. 12, no. 1, Dec. 2010, Art. ID 015005.
[9] Y. Zhang, L. Xia, C. Zhou, X. Yu, H. Liu, D. Liu, and Y. Zhang, “Microstructured fiber based plasmonic index sensor with optimized accuracy and calibration relation in large dynamic range,” *Opt. Commun.*, vol. 284, no. 18, pp. 4161–4166, Aug. 2011.
[10] Y. Peng, J. Hou, Z. Huang, and Q. Lu, “Temperature sensor based on surface plasmon resonance within selectively coated photonic crystal fiber,” *Appl. Opt.*, vol. 51, no. 26, pp. 6361–6367, Sep. 2012.
[11] N. Luan, R. Wang, Y. Lu, and J. Yao, “Simulation of surface plasmon resonance temperature sensor based on liquid mixture-filling microstructured optical fiber,” *Opt. Eng.*, vol. 53, no. 6, Jun. 2014, Art. ID 067103.
[12] N. Luan, R. Wang, Y. Lu, and J. Yao, “Surface plasmon resonance temperature sensor based on photonic crystal fibers randomly filled with silver nanowires,” *Sensors*, vol. 14, no. 9, pp. 16035–16045, Aug. 2014.
[13] B. H. Liu, Y. X. Jiang, X. S. Zhu, X. L. Tang, and Y. W. Shi, “Hollow fiber surface plasmon resonance sensor for the detection of liquid with high refractive index,” *Opt. Express*, vol. 21, no. 26, pp. 32549-32557, Dec. 2013.

1943-0655(c) 2016 IEEE. Translations and content mining are permitted for academic research only. Personal use is also permitted, but republication/redistribution requires IEEE permission. See http://www.ieee.org/publications_standards/publications/rights/index.html for more information.

This article has been accepted for publication in a future issue of this journal, but has not been fully edited. Content may change prior to final publication. Citation information: DOI 10.1109/JPHOT.2017.2694479, IEEE Photonics Journal

[14] N. Luan and J. Yao, "High refractive index surface plasmon resonance sensor based on a silver wire filled hollow fiber," *IEEE Photonics J.*, vol. 8, no. 1, Feb. 2016, Art. ID 4800709.
[15] H. W. Lee, M. A. Schmidt, H. K. Tyagi, L. P. Sempere, and P. St. J. Russell, "Polarization-dependent coupling to plasmon modes on submicron gold wire in photonic crystal fiber," *Appl. Phys. Lett.*, vol. 93, no. 11, Sep. 2008, Art. ID. 111102.
[16] M. A. Schmidt, L. N. P. Sempere, H. K. Tyagi, C. G. Poulton, and P. St. J. Russell, "Waveguiding and plasmon resonances in two-dimensional photonic lattices of gold and silver nanowires," *Phys. Rev. B.*, vol. 77, no. 3, Jan. 2008, Art. ID. 033417.
[17] A. Nagasaki, K. Saitoh, and M. Koshiba, "Polarization characteristics of photonic crystal fibers selectively filled with metal wires into cladding air holes," *Opt. Express*, vol. 19, no. 4, pp. 3799–3808, Feb. 2011.
[18] M. A. Schmidt and P. St. J. Russell, "Long-Range spiralling surface plasmon modes on metallic nanowires," *Opt. Express*, vol. 16, no. 18, pp. 13617–13623, Sep. 2008.
[19] H. W. Lee, M. A. Schmidt, R. F. Russell, N. Y. Joly, H. K. Tyagi, P. Uebel, and P. St. J. Russell, "Pressure-assisted melt-filling and optical characterization of Au nano-wires in microstructured fibers," *Opt. Express*, vol. 19, no. 13, pp. 12180–12189, Jun. 2011.
[20] H. K. Tyagi, H. W. Lee, P. Uebel, M. A. Schmidt,N. Joly, M. Scharrer, and P. St. J. Russell, "Plasmon resonances on gold nanowires directly drawn in a step-index fiber," *Opt. Lett*., vol. 35, no. 15, pp. 2573–2575, Aug. 2010.
[21] P. J. A. Sazio, A. Amezcua-Correa, C. E. Finlayson, J. R. Hayes, T. J. Scheidemantel, N. F. Baril, B. R. Jackson, D. J. Won, F. Zhang, E. R. Margine, V. Gopalan, V. H. Crespi, and J. V. Badding, "Microstructured optical fibers as high-pressure micro fluidic reactors," *Science*, vol. 311, no. 5767, pp. 1583–1586, Mar. 2006..
[22] J. A. Harrington, "A review of IR transmitting, hollow waveguides," *Fiber Integr. Opt.*, vol. 19, no. 3, pp. 211–227, 2000.
[23] A. D. Rakić, A. B. Djurišić, J. M. Elazar, and M. L. Majewski, "Optical properties of metallic films for vertical-cavity optoelectronic devices," *Appl. Opt*., vol. 37, no. 22, pp. 5271–5283, Aug. 1998.
[24] X. Zhang, R. Wang, F. M. Cox, B. T. Kuhlmey, and M. C. J. Large, "Selective coating of holes in microstructured optical fiber and its application to in-fiber absorptive polarizers," *Opt. Express*, vol. 15, no. 24, pp. 16270–16278, Nov. 2007.
[25] N. Luan, R. Wang, W. Lv, and J. Yao, "Surface plasmon resonance sensor based on exposed-core microstructured optical fibres," *Electron. Lett*., vol. 51, no. 9, pp. 714–715, Apr. 2015.

1943-0655 (c) 2016 IEEE. Translations and content mining are permitted for academic research only. Personal use is also permitted, but republication/redistribution requires IEEE permission. See http://www.ieee.org/publications_standards/publications/rights/index.html for more information.